

A 2-20 GHz, HIGH-GAIN, MONOLITHIC HEMT DISTRIBUTED AMPLIFIER*

C. Nishimoto, R. LaRue, S. Bandy, M. Day, J. Eckstein,
C. Webb, C. Yuen and G. Zdasiuk

Varian Research Center
Device Laboratory
Palo Alto, CA 94303

ABSTRACT

A low-noise 2-20 GHz monolithic distributed amplifier utilizing 0.3-micron gate-length HEMT devices has achieved $11\text{ dB} \pm 0.5\text{ dB}$ of gain. This represents the highest gain reported for a distributed amplifier using single FET gain cells. A record low noise figure of 3 dB was achieved mid-band (7-12 GHz). The circuit design utilizes five HEMT transistors of varying width with gates fabricated by E-beam lithography.

INTRODUCTION

While a number of authors have reported reactively-tuned, narrow-band gains and noise figures for discrete high electron mobility transistors (HEMT) [1-2], this paper is the first to report results of a working monolithic distributed amplifier utilizing 0.3-micron gate-length HEMTs. Also, many workers have reported monolithic distributed amplifiers utilizing 0.5-micron gate-length MESFETs that have achieved 7-8 dB gain and approximately 5-dB noise figure in the 2-20 GHz band [3]. By replacing the conventional MESFET with high-performance, 0.3-micron gate-length HEMTs, significant improvements in gain and noise figure are achievable. From the circuit design point of view, HEMTs possess significant differences when compared to MESFETs. As shown in Fig. 1, the HEMT AlGaAs epitaxial layer is doped higher than the active layer in a MESFET, and the HEMT usually possesses higher intrinsic transconductance, as high as 500 mS/mm but with a concomitant higher gate capacitance. Additionally, the gate to drain breakdown voltage for the HEMT may be reduced because of the higher doping, impacting the power performance.

CIRCUIT DESIGN

Figure 2 shows the equivalent circuit model for discrete, 0.3-micron gate-length HEMTs fabricated in our lab. The devices were first char-

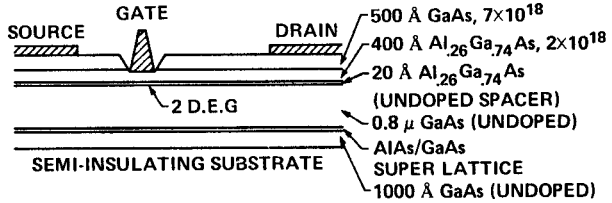


Fig. 1 Cross section of high electron mobility transistor fabricated in the lab. A noise figure of 1.35 dB and associated gain of 12 dB were measured at 18 GHz.

acterized by s-parameter measurements in the common-gate, common-source, and common-drain configurations from 2-18 GHz. A single equivalent circuit model is then constrained to fit the three sets of data. Details of the procedure are described elsewhere [4], but it should be noted that this particular device had a g_m of 520 mS/mm. Because the doping is high, C_{gs} is expected to be high, but is kept to a minimum by reducing the gate length.

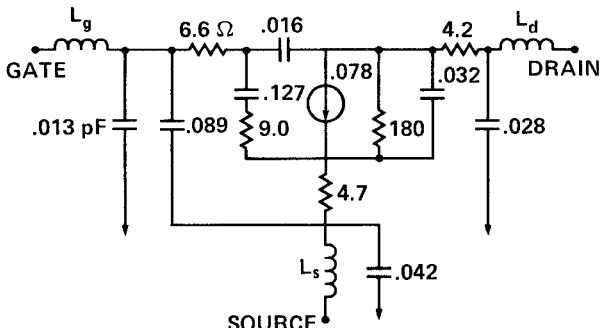


Fig. 2 Equivalent circuit model of HEMT device. The intrinsic transconductance was found to be 520 mS/mm.

*This work supported by Naval Air Development Center under NRL Contract N00014-86-C-2048.

The equivalent circuit of Fig. 2 was used in the design of a five-HEMT distributed amplifier in the 2-20 GHz band. CAD was used to optimize 24 circuit design parameters including five HEMT gate widths and twelve gate and drain line lengths. By allowing the HEMTs to vary in width and the gate and drain line sections to vary in length, the gain is enhanced by 1-2 dB and an improved return loss is achieved when compared to the conventional constant-K design. Additional details of this variable device width design approach are found elsewhere [4], but generally the wider HEMTs are located in the center of the amplifier or near the gate line termination. The total HEMT periphery is 720 microns. A photomicrograph of the complete chip is shown in Fig. 3. Note the variable lengths of the gate and drain line sections. This MMIC also has on-chip gate and drain line terminations and gate and drain biasing networks.

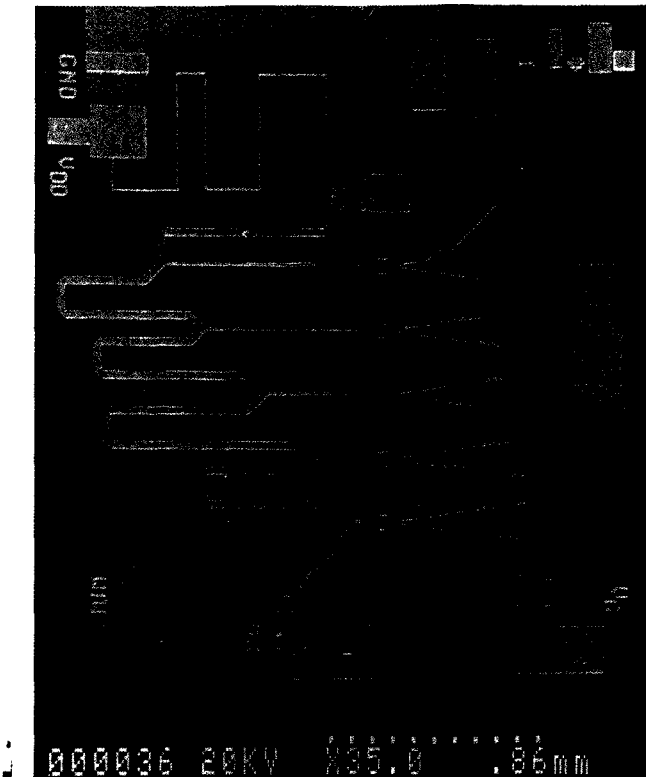


Fig. 3 Photomicrograph of HEMT amplifier. Chip size: 3.0 mm x 2.4 mm.

FABRICATION

The HEMT layers shown in Fig. 1 were grown by MBE at 565°C. The GaAs is unintentionally doped n-type at about $1 \times 10^{14}/\text{cm}^3$. A five-period AlAs/GaAs superlattice is grown midway into the buffer layer in an attempt to reduce dislocations and improve surface morphology.

Standard processing techniques were used for most of the HEMT distributed amplifier fabrication. Isolation was achieved with a 2500 Å mesa etch. Figure 4 shows a photomicrograph of a typical submicron gate fabricated in the lab using

E-beam lithography. Gate exposures in PMMA were achieved with an automated SEM, after which a shallow gate etch to the first layer of AlGaAs was performed. In order to achieve good grounding of the source, 50 x 50-micron backside vias were incorporated using reactive ion etching. All other process steps used conventional metallization, liftoff and pulse plating techniques.



Fig. 4 Photomicrograph of gate and gate lead of a typical submicron HEMT device.

MEASURED GAIN PERFORMANCE

As shown in Fig. 3, the layout of the circuit is compatible with RF wafer probing techniques. Figure 5 shows the gain and return loss obtained using the Cascade Microtech rf wafer prober. 11 dB \pm 0.5 dB of gain over the 2-18 GHz bandwidth was achieved. The drain and gate bias were adjusted for optimum performance ($V_d = 4.0$ V, $V_{gs} = -0.66$ V).

The HEMT device is particularly suited for achieving high gain in distributed amplifiers because of its higher transconductance and lower output conductance compared with MESFETs. The higher transconductance comes about as a result of the saturated velocity [5,6], and the fact that AlGaAs can be doped higher than GaAs without compromising the gate breakdown voltage (by virtue of its larger bandgap). The lower output conductance is a result of the two-dimensional nature of the conduction electrons.

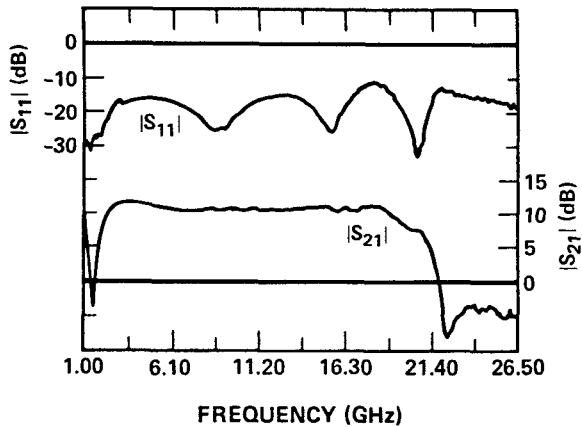


Fig. 5 Gain and return loss of working HEMT amplifier. $V_{ds} = 4$ V, $V_{gs} = -0.6$ V, $I_{ds} = 151$ mA.

Ignoring feedback, the maximum gain of a reactively-matched FET is given by

$$G \approx \frac{g_m^2}{4\omega^2 C_{gs}^2 r_i g_{ds}}$$

while that for a distributed amplifier is given by

$$G \approx \frac{g_m^2 R_o^2}{4} \left(\frac{1}{1 + g_{ds} R_o} \right),$$

with r_i the input resistance, g_{ds} the output conductance, and R_o the characteristic impedance of the transmission lines. With C_{gs} , $g_{ds} \propto g_m$ and $r_i \propto g_m^{-1}$, the reactively-matched gain does not have a strong dependence upon g_m .

On the other hand, for $g_{ds} R_o \ll 1$, the distributed amplifier gain is proportional to g_m^2 provided that C_{gs} does not become so high as to compromise achieving the desired values of R_o and transmission line cutoff frequency, f_c . The HEMT device thus takes better advantage of its higher transconductance in a distributed rather than a reactively-matched amplifier setting.

While it is true that the small 0.3-micron gate lengths are partially responsible for the improved performance of Fig. 5, simulations show that the deterioration of g_{ds} with decreasing gate length results in only marginal gain improvement with MESFETs using such small gate lengths. This necessitates going to a scheme like the cascode configuration [4] to circumvent this problem. The lower output conductance of the HEMT device enables the advantages of a shorter gate length to be realized in the distributed amplifier configuration without resorting to a more complicated gain cell. Simulations using the HEMT device in the

cascode configuration indicate gains of 15 dB over the 2-20 GHz bandwidth can be achieved.

When biased at maximum gain ($V_{ds} = 4$ V, $I_{ds} = 151$ mA), the 1-dB compressed power was measured to be 14 dBm at 10 GHz. The third-order intermodulation intercept point was measured to be 23 dBm under the same conditions. The 9-dB difference between these two measurements is less than the theoretical difference of 10.6 dB [7], but equal to the 8-9 dB difference seen for MESFETs. For the same bias current and voltage, MESFET distributed amplifiers have around 5-dB higher compressed power and third-order intercept levels when biased for maximum gain. Presumably, the lower values for the HEMT version are due to a much higher nonlinearity in the g_m versus gate bias characteristic.

AMPLIFIER NOISE PERFORMANCE

This section will discuss HEMT low-noise performance, HEMT suitability for broadband low-noise applications, and the measured noise performance of the distributed amplifier.

The narrowband noise performance of discrete HEMT devices fabricated in our facility is typically a minimum noise figure of 1.25 to 1.5 dB at 18 GHz, with an associated gain of 11-12 dB for gate lengths in the 0.3-0.35 micron range.

The noise figure of a FET device can be expressed by [9]

$$F = 1 + \frac{r_n}{R_s} + \frac{g_n}{R_s} \left[\left(R_s + \sqrt{R_s^2 - \frac{r_n}{g_n}} \right)^2 + (X_s - X_{s,opt})^2 \right]$$

where r_n and g_n are the noise resistance and conductance, respectively, $Z_s = R_s + jX_s$ is the source impedance, and $R_{s,opt} + jX_{s,opt}$ is the optimum source impedance for minimum noise. The equation shows that, under conditions of noise mismatch such as encountered in a distributed amplifier, the largest noise bandwidths occur when g_n and the ratio $X_{s,opt}/R_{s,opt}$ are the smallest. Empirical data has been taken [9] which demonstrate that HEMT devices have lower values of both g_n and the ratio $X_{s,opt}/R_{s,opt}$ in comparison to MESFETs. Accordingly, HEMT devices should be better suited for broadband low-noise applications.

Figure 6 compares the gate bias dependence of the minimum noise figure and associated gain at 12.4 GHz for both the HEMT and MESFET devices in a 50-ohm system (no input or output matching) which gives some indication of what would be experienced in the 25-ohm environment of a distributed amplifier. Both FETs have a 0.4-micron gate length and the HEMT has a 50 Å AlGaAs spacer layer. The HEMT has an advantage of approximately 1 dB in both the minimum noise figure and the associated gain under these conditions.

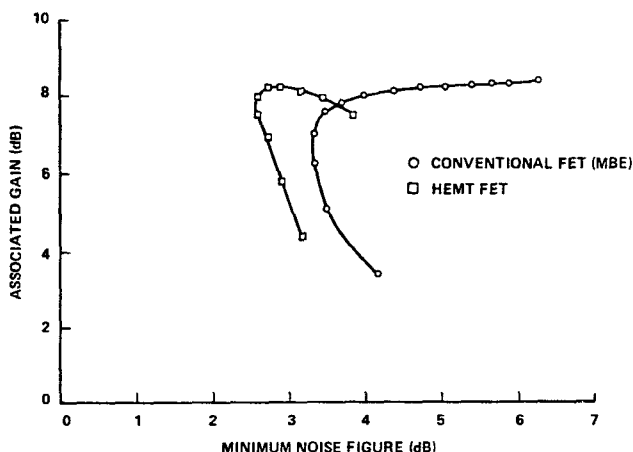


Fig. 6 12-GHz FET performance in a 50-ohm system.

Figure 7 shows the minimum noise performance for the amplifier. The low value of approximately 3 dB over the 7-12 GHz midband region exceeds previously reported performance for distributed amplifiers by several dB for the same bandwidth [3,10,11]. The associated gain of around 10.5 dB is quite close to the maximum gain by virtue of the small difference between the gate biases for maximum gain and minimum noise ($I_{ds} = 151$ mA versus 131 mA). Figure 7 shows the usual noise skirts due to the gate termination resistor on the low frequency end and the transmission line cutoff frequency on the high end of the band. The maximum gain bias yields virtually the same noise performance, having the same 3-dB midband performance with the rise at the high end of the band being only 0.3 dB higher.

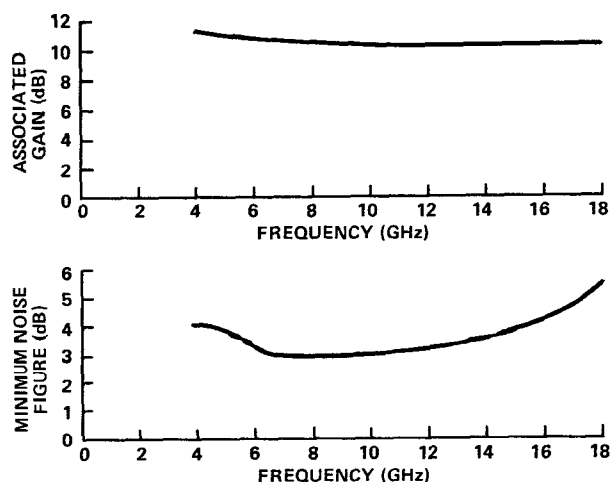


Fig. 7 Noise performance of the HEMT amplifier.
 $V_{ds} = 4$ V, $V_{gs} = -0.71$ V, $I_{ds} = 131$ mA.

The amplifier was designed for maximum gain rather than minimum noise figure for purposes of achieving a multistage gain of 20 dB with as few stages as possible. Optimization using the considerations in Ref. 12 in conjunction with a suitable computer simulation program for noise sources should give a design which reduces the noise figure further.

CONCLUSION

The results presented in this paper indicate that by using high-performance, low-noise HEMTs with gates defined by E-beam lithography, record improvements in gain and noise figure can be achieved for broadband distributed amplifiers. A gain of $11 \text{ dB} \pm 0.5 \text{ dB}$ from 2-18 GHz and a midband noise figure of 3 dB have been achieved on a working HEMT amplifier. This represents the highest gain and lowest noise figure reported for a distributed amplifier using single FETs for the gain cell. The HEMT device is able to outperform its MESFET counterpart with the same gate length in distributed amplifier applications by virtue of its higher transconductance and lower output conductance.

REFERENCES

1. M. Sholley and A. Nichols, "60 and 70 GHz (HEMT) Amplifiers", 1986 IEEE MTT-S Digest, p. 463.
2. J. J. Berenz, W. Nakamo, K. Weller, "Low Noise High Electron Mobility Transistors", 1984 IEEE MTT-S Digest, p. 83.
3. T. McKay, J. Eisenberg and R. E. Williams, "A High-Performance 2-18.5 GHz Distributed Amplifier -- Theory and Experiment", IEEE Trans. Microwave Theory Tech. MTT-34, 1559 (1986).
4. R. A. LaRue et al., "A 12-dB High-Gain Monolithic Distributed Amplifier", IEEE Trans. Microwave Theory Tech. MTT-34, 1542 (1986).
5. T. J. Drummond et al., "Enhancement of Electron Velocity in Modulation-Doped (Al_xGa_{1-x})As/GaAs FETs at Cryogenic Temperatures", Electron. Lett. 18, 1057 (1982).
6. T. Hanoguchi and O. Miyatsuji, "Negative Differential Mobility and Velocity Overshoot", Eng. Foundation Second SDHT Conf., Hawaii, Dec. 1986.
7. G. L. Heiter, "Characterization of Nonlinearities in Microwave Devices and Systems", IEEE Trans. Microwave Theory Tech. MTT-21, 797 (1973).
8. R. A. Pucell, H. A. Haus and H. Stutz, "Signal and Noise Properties of Gallium Arsenide Microwave Field Effect Transistors", in Advances in Electronics and Electron Physics, ed. L. Marton (Academic Press, NY, 1975), Vol. 38, p. 195.

9. S. Weinreb and M. Pospiezalski, "X-Band Noise Parameters of HEMT Devices at 300K and 12.5K", 1985 IEEE MTT-S Digest, p. 539.
10. W. Kennan, T. Andrade and C. C. Huang, "A 2-18 GHz Monolithic Distributed Amplifier Using Dual-Gate GaAs FETs", IEEE Trans. Electron. Devices ED-31, 1926 (1984).
11. Y. Ayasli, et al., "2-20 GHz GaAs Traveling-Wave Amplifier", IEEE Trans. Microwave Theory Tech. MTT-32, 71 (1984).
12. K. B. Niclas and B. A. Tucker, "On Noise in Distributed Amplifiers at Microwave Frequencies", IEEE Trans. Microwave Theory Tech. MTT-31, 661 (1983).